Acta Oceanol. Sin., 2017, Vol. 36, No. 10, P. 8–19
DOI: 10.1007/s13131-017-1068-1
http://www.hyxb.org.cn
E-mail: hyxbe@263.net

Biomarker assessments of sources and environmental implications of organic matter in sediments from potential cold seep areas of the northeastern South China Sea

DING Ling[1, 2], ZHAO Meixun[1]*, YU Meng[1], LI Li[1], HUANG Chi-Yue[3]

[1] Key Laboratory of Marine Chemistry Theory and Technology (Ocean University of China), Ministry of Education, Qingdao 266100, China

[2] Key Laboratory of Marine Hydrocarbon Resources and Environmental Geology, Ministry of Land and Resources, Qingdao 266071, China

[3] Department of Earth Sciences, National Cheng Kung University, Tainan 701, Taiwan, China

Received 13 April 2016; accepted 2 November 2016

Abstract

Multi-biomarker indexes were analyzed for two piston cores from potential cold seep areas of the South China Sea off southwestern Taiwan. Total organic carbon (TOC) normalized terrestrial (*n*-alkanes) and marine (brassicasterol, dinosterol, alkenones and *iso*-GDGTs) biomarker contents and ratios (TMBR, $1/P_{\text{mar-aq}}$, BIT) were used to evaluate the contributions of terrestrial and marine organic matter (TOM and MOM respectively) to the sedimentary organic matter, indicating that MOM dominated the organic sources in Core MD052911 and the sedimentary organic matter in Core ORI-860-22 was mainly derived from terrestrial inputs, and different morphologies were the likely reason for TOM percentage differences. BIT results suggested that river-transported terrestrial soil organic matter was not a major source of TOM of sedimentary organic matter around these settings. Diagnostic biomarkers for methane-oxidizing archaea (MOA) were only detected in one sample at 172 cm depth of Core ORI-860-22, with abnormally high *iso*-GDGTs content and Methane Index (MI) value (0.94). These results indicated high anaerobic oxidation of methane (AOM) activities at or around 172 cm in Core ORI-860-22. However in Core MD052911, MOA biomarkers were not detected and MI values were lower (0.19–0.38), indicated insignificant contributions of *iso*-GDGTs from methanotrophic archaea and the absence of significant AOM activities. Biomarker results thus indicated that the discontinuous upward methane seepage and insufficient methane flux could not induce high AOM activities in our sampling sites. In addition, the different patterns of TEX_{86} and $U^{K'}_{37}$ temperature in two cores suggested that AOM activities affected TEX_{86} temperature estimates with lower values in Core ORI-860-22, but not significantly on TEX_{86} temperature estimates in Core MD052911.

Key words: biomarkers, organic matter sources, TOM, MOM, anaerobic oxidation of methane, South China Sea

Citation: Ding Ling, Zhao Meixun, Yu Meng, Li Li, Huang Chi-Yue. 2017. Biomarker assessments of sources and environmental implications of organic matter in sediments from potential cold seep areas of the northeastern South China Sea. Acta Oceanologica Sinica, 36(10): 8–19, doi: 10.1007/s13131-017-1068-1

1 Introduction

Gas hydrate is a crystalline solid composed of methane and water molecule and it is potentially an important energy source. As a greenhouse gas, methane can be released from gas hydrate and subsequently can migrate upward along geological fractures. However, this migration process is very slow, and most of the upward moving methane is oxidized in the interior or surface sediments and recycled in anoxic marine sediments (Reeburgh et al., 1991; Reeburgh, 2007). Anaerobic oxidation of methane (AOM) mediated by consortia of methane-oxidizing archaea (MOA) and sulfate-reducing bacteria (SRB) (Hoehler et al., 1994; Boetius et al., 2000; Orphan et al., 2001; Pancost et al., 2001), has been recognized as a key process controlling the biogeochemical cycle of methane in cold seep sediments, and is of major relevance for the global balance of methane (Pape et al., 2005; Reeburgh, 2007; Wegener and Boetius, 2009). Moreover, archaeal community mediated AOM also plays an important role in other deep sea biogeochemical cycles, including both methanogenesis and nutrient recycling (Kaneko et al., 2013). Due to the additional organic compounds synthesized by MOA and methanogenesis, the distribution and compositon of organic matter in cold seep sediments may be more complicated than that in normal sediments.

Large-scale coring projects have been undertaken to estimate the potential of gas hydrate reservoirs in the active continental margin off southwestern (SW) Taiwan, and geophysical and geochemical data both indicated that gas hydrates distribute widely in sediments of this area (Chi et al., 1998; Chuang et al., 2006; Huang et al., 2006a; Lin et al., 2006; Liu et al., 2006). Seismic surveys revealed the wide occurrences of strong Bottom Simulating Reflector (BSR) beneath the seafloor offshore SW Taiwan (Chi et al., 1998; Liu et al., 2006), and geochemical studies discovered that sulfate reducing zones were as shallow as ~1 m be-

Foundation item: The National Natural Science Foundation of China under contract No. 41521064; the Key Laboratory of Marine Hydrocarbon Resources and Environmental Geology under contract No. MRE201301.
*Corresponding author, E-mail: maxzhao@ouc.edu.cn

neath the sediment-water interface with high upward methane flux (Lin et al., 2006). Detailed studies for methane concentration of bottom waters and sediment pore waters showed that some sites with extremely high methane concentrations existed in the syn-collision accretionary prism of the Kaoping Slope off Taiwan (Chuang et al., 2006). Studies on biological and mineralogical components of surface and core sediments retrieved from the Kaoping Slope found that the occurrences of tubeworms, pyrites and authigenic carbonates with highly depleted carbon isotope values corresponded to high methane concentrations in bottom water (Huang et al., 2006a). All of the studies above demonstrated that there are active cold seeps with methane expulsion from the Kaoping Slope.

Organic geochemical studies using biomarkers have been widely applied for cold seeps to provide evidence of AOM, but this approach has not been used in the Kaoping Slope region. Microbes are the basis of cold seep ecosystem, and consortia of MOA and SRB mediated AOM can generate a series of lipid biomarkers, i.e., crocetane, pentamethylicosane (PMI), archaeol, *sn*-2-/*sn*-3-hydroxyarchaeol, glycerol dibiphytanyl glycerol tetraethers (GDGTs), DGDs and fatty acids (Elvert et al., 1999; Hinrichs et al., 2000; Hopmans et al., 2000; Zhang et al., 2002; Bouloubassi et al., 2006; Stadnitskaia et al., 2008). Lipid biomarkers become a significant geochemical method on cold seep research; and their type, content and stable carbon isotopic compositions ($^{13}C/^{12}C$) can indicate the existence of microorganisms and can also provide important information on the variations of microbial community structures at contemporary and ancient methane-seeps (Elvert et al., 1999; Bian et al., 2001; Pancost et al., 2001; Pancost and Damste, 2003; Elvert et al., 2005; Pape et al., 2005; Guan et al., 2013). However, it has been adopted in only a few AOM settings characterized by diffusive supply of methane, partly because high allochthonous OM inputs tend to obscure the occurrence of biomarkers derived from organisms involved in AOM (Biddle et al., 2006; Parkes et al., 2007; Aquilina et al., 2010).

Here, we report several organic geochemical indexes of two piston cores collected from the SW Taiwan continental margin. Multiple biomarkers originated from higher plants, marine phytoplankton, and in particular AOM-performing biomarkers were analyzed to assess the relationships between biomarkers distribution patterns and local depositional settings, and AOM process in the Kaoping Slope off SW Taiwan.

2 Materials and methods

2.1 *Geological settings and sampling*

The area offshore SW Taiwan locates in the transition zone of the Luzon Arc and the China passive continental margin subduction-collision system (Liu et al., 2004). The Kaoping Slope representing an accretionary prism has been developing since the late Miocene during the collision between the Luzon volcanic arc of the Philippine Sea Plate and the Asia continental margin of the Eurasian Plates (Huang et al., 2006b). A series of normal faults in this accretionary prism can provide good conduits for gas and fluid venting upward to the surface (Lin et al., 2006). In view of the geological characters of the Kaoping Slope, many investigations have been performed to assess potential active cold seep sites (Chi et al., 1998; Chuang et al., 2006; Huang et al., 2006a; Lin et al., 2006; Liu et al., 2006). Noticeably, this area also receives a high flux of terrigenous suspended sediments exported from the adjacent Kaoping (49.0 Mt/a), Erjen (30.2 Mt/a) and Tsengwen (25.1 Mt/a) rivers with a combined river particle load of 104 Mt/a (Dadson et al., 2003).

Remotely operated vehicle (ROV) surveys and sediment sampling were conducted during 2004–2007 in the Kaoping Slope (Fig. 1). On the base of these surveys, this study focused on two piston cores collected from high potential cold seep sites at the Kaoping Slope. Giant piston Core MD052911 (22°15.61′N, 119°51.08′E; 1 076 m water depth) was retrieved in 2005 by R/V *Marion Dufrense*. The length of Core MD052911 is 2 389 cm, and 29 samples from 294 cm to 809 cm depth were taken at 2–3 cm intervals for organic geochemical analysis, where the CH_4 concentration varied significantly (Yang T F, personal communication). Another piston Core ORI-860-22 (22°13.08′N, 119°50.63′E; 1 237 m water depth) was taken from the Good Weather Ridge during R/V *OR-I*, a cruise of chemosynthetic community investigation in 2007 by Taiwanese and Japanese scientists. The length of Core ORI-860-22 is 251 cm, and 24 samples from 16 cm to 235 cm depth were taken at 2 cm intervals and analyzed, crossing the sulphate-methane transition zone (Yang T F, personal communication).

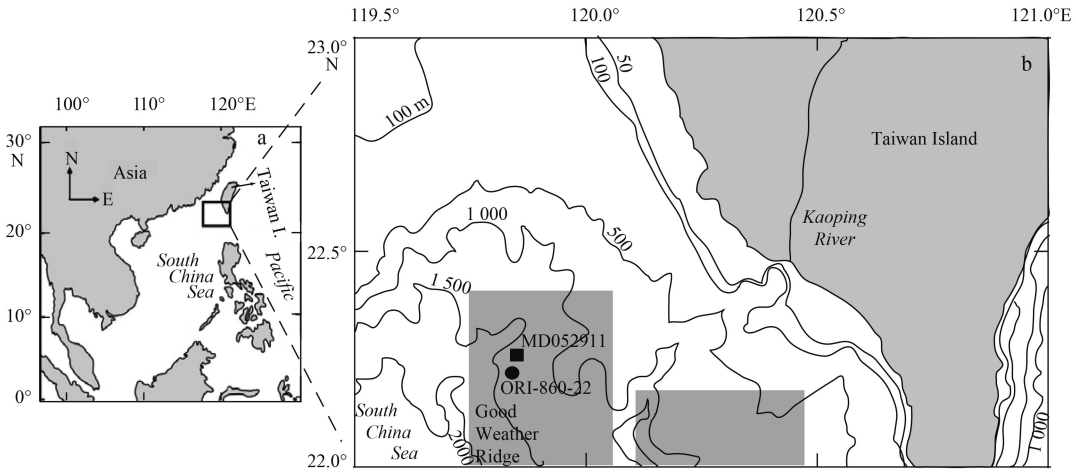

Fig. 1. A map showing the study area in the South China Sea (a), and site locations of MD052911 (filled square) and ORI-860-22 (filled circle) (b) (Chen et al., 2011). Two gray rectangles in Fig. b denote promising areas of cold seeps from Liu et al. (2006) and Huang et al. (2006a).

2.2 *Methods*

2.2.1 *TOC*

Total organic carbon (TOC) contents were measured by high temperature combustion on a Thermo Flash 2000 Elemental Analyzer. Sediment samples were acidified with 4 mol/L HCl at room temperature to remove inorganic carbon. After rinsing with Milli-Q water several times and drying in an oven at 55°C, the carbonate-free samples were measured for TOC with a standard deviation of ±0.02 wt% determined by replicated analysis (n=6).

2.2.2 *Biomarkers extraction*

Sediments were freeze-dried and homogenized by a mortar and a pestle. 5–6 g (dry mass) homogenized sediments in Teflon bottles were extracted four times by ultrasonication after adding internal standards. Because most of the cold seep samples were especially rich in elemental sulfur, active copper was added to remove elemental sulfur from the total extracts. The supernatants were collected, and after evaporation of the solvents, an aliquot of the total lipid extracts was hydrolyzed with 6% KOH/methanol. Neutral lipids containing biomarkers were extracted with n-hexane and then further fractionated into apolar (alkanes) and polar (alkenones, sterols and GDGTs) fractions using a solid phase extraction step with a silica gel column and different eluents. The apolar fraction containing alkanes was condensed under a stream of nitrogen and dissolved in 30 μL isooctane before gas chromatography (GC) analysis. Part of the polar fraction containing sterols and alkenones was condensed and derivatized with N, O-bis (trimethylsily)-trifluoroacetamide (BSTFA) before injection into the GC; the rest containing GDGTs was redissolved in 500 μL isopropanol-hexane and filtered using a PTFE 0.45 μm filter prior to injection in the HPLC-MS.

2.2.3 *Gas chromatography, GC-IRMS and HPLC-MS analysis*

Two fractions containing alkanes, sterols and alkenones were analyzed for lipid biomarker contents using GC (Agilent 6890), equipped with a silica capillary column (HP-1 Methyl Siloxane, 50 m, 0.32 mm i.d. and 0.17 μm film thickness) and a flame ionization detector. For alkanes detection, hydrogen was used as carrier gas with a flow rate of 1.0 mL/min. The temperature program was 80°C for 1 min, heating with a rate of 25°C/min to 200°C, then followed successively by 1.5°C/min to 230°C, 2°C/min to 250°C, 5°C/min to 300°C (maintained for 1 min), and 5°C/min to 310°C (maintained for 10 min). For sterols and alkenones detection, hydrogen was used as the carrier gas with a flow rate of 1.1 mL/min. The column temperature was programmed from 80°C to 200°C at 25°C/min, then followed successively by 4°C/min to 250°C, 1.8°C/min to 300°C (maintained for 15 min), and 5°C/min to 310°C (maintained for 8 min). Selected samples were examined by GC-MS for compound identification operating under the same conditions as GC analysis described above.

n-Alkanes of representative samples were measured for their stable carbon isotopic compositions ($^{13}C/^{12}C$) using a GC-IRMS system, which consists of a Thermo Trace GC ULTRO coupled to a Thermo Delta V isotope ratio mass spectrometry via a GC-C III interface. The DB-1 MS capillary column (60 m, 0.25 mm i.d. and 0.25 μm film thickness) was used for alkanes separation, and helium was used as the carrier gas with a flow rate of 1.0 mL/min. Oven temperature was programmed at a rate of 15°C/min from 60 to 200°C, then followed by 4°C/min to 250°C, 1.8°C/min to 300°C, 5°C/min to 310°C (maintained for 5 min). n-Alkanes separated by GC were oxidized to CO_2 at 980°C that was continuously introduced into the mass spectrometer ion source for stable isotope analysis. $^{13}C/^{12}C$ were reported in the delta notation ($\delta^{13}C$) calibrated to the Peedee belemnite (PDB) standard. A set of C_{15} n-alkanes with known $\delta^{13}C$ values were measured daily to ensure the accuracy of ±0.5‰.

GDGTs analysis was performed using an Agilent 1200 series HPLC coupled to a Waters Micromass-Quattro Ultima™ Pt mass spectrometer equipped with an APCI probe. Separation was achieved on a Prevail Cyano Column (150 mm×2.1 mm, 3 μm), maintained at 30°C. GDGTs were eluted isocratically with hexane and hexane/isopropanol (9:1, v/v), with a flow rate 0.3 mL/min. Conditions for the APCI-MS were: corona 6 μA, source temperature 95°C, cone 35 V, APCI probe temperature 550°C, cone gas (N_2) flow 90 L/h, desolvation gas (N_2) flow 600 L/h. Selected Ion Recording (SIR) was used to detect the protonated molecules $[M+H]^+$ (dwell time=50 ms) of GDGTs (m/z 1 302, 1 300, 1 298, 1 296, 1 292, 1 050, 1 036, 1 022, 744 (C_{46} GDGT, internal standard)).

3 Results

3.1 *Terrestrial and marine biomarkers*

C_{23} to C_{33} n-alkanes were found in all samples, with a strong odd to even number predominance and maximizing at n-C_{29} or n-C_{31}. Two representative partial gas chromatograms of the hydrocarbon fractions are shown in Fig. 2. Biomarker content was normalized to TOC content in order to minimize the effect of varying sedimentation rate and degradations. The TOC normalized content of n-alkanes (C_{27}+C_{29}+C_{31}) in Core MD052911 varied from 688 to 1 215 ng/g with an average value of 971 ng/g; and the TOC normalized content in Core ORI-860-22 ranged from 1 387 to 2 126 ng/g with an average value of 1 674 ng/g (Fig. 3). From 807.5 cm to 545 cm depth in MD052911, the n-alkane (C_{27}+C_{29}+C_{31}) content decreased and reached a minimum, then increased and reached a maximum around 349 cm (Fig. 3a). In ORI-860-22 samples, n-alkane content increased gradually from the bottom and reached a maximum at 81 cm depth, afterward it began a decreasing trend toward the coretop (Fig. 3b).

A series of sterols and alkenones were detected in most sediment samples. Figure 4 shows partial chromatograms of the neutral fractions (aliphatic alcohols and alkenones) from Cores MD052911 (Fig. 4a) and ORI-860-22 (Fig. 4b). TOC normalized sum content of the three marine phytoplankton biomarkers (∑MB=brassicasterol+dinosterol+C_{37}-alkenones) in Core MD052911 varied from 844 to 2 123 ng/g with an average value of 1 598 ng/g, and the sum in Core ORI-860-22 ranged from 988 to 1 937 ng/g with an average value of 1 343 ng/g (Fig. 3). For Core MD052911, depth profiles of phytoplankton biomarkers showed similar trends (Fig. 3a), with minimum values at around 550 cm depth. After that, the biomarker contents generally increased toward the coretop. In Core ORI-860-22, brassicasterol and dinosterol contents also varied similarly, with generally higher values from 234 to 175 cm and lower values from 175 cm to the coretop (Fig. 3b). Alkenone content showed a different trend, with two higher value intervals at 234–200 cm and around 125 cm (Fig. 3b).

The $U^{K'}_{37}$ index is used to estimate sea surface temperatures (SST) by using Müller's global equation (Eqs (1) and (2)) (Müller et al., 1998). $U^{K'}_{37}$-SST varied from 20.5°C to 25°C for Core MD052911 with an average of 23.8°C, while the range of SST variations in Core ORI-860-22 was 20.8°C to 23.7°C with an average of 22.8°C.

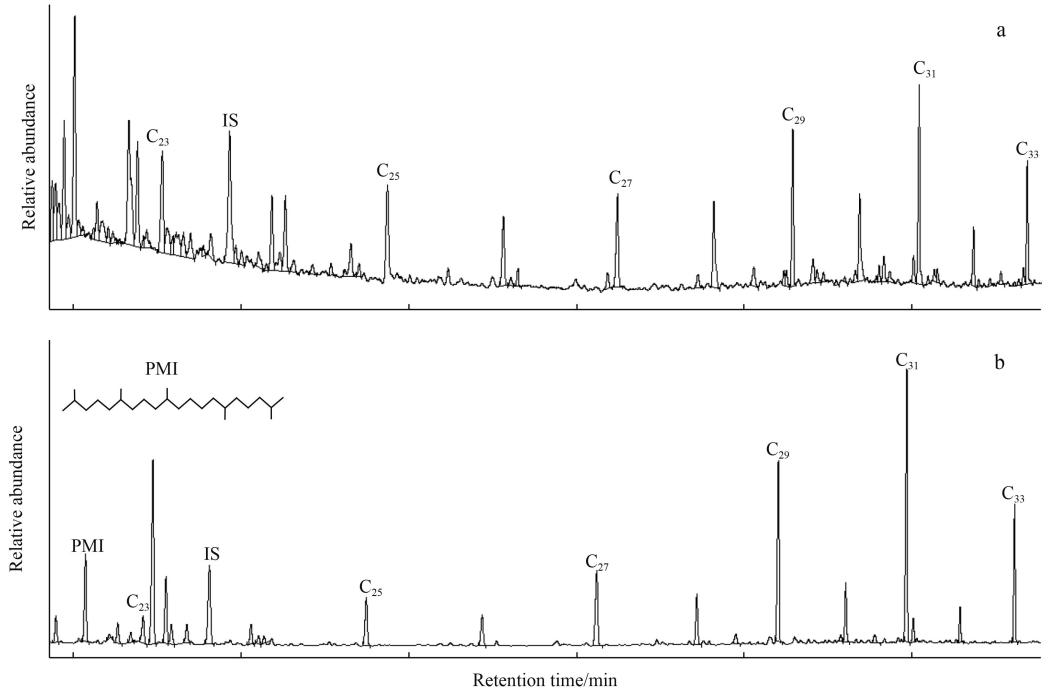

Fig. 2. Partial gas chromatograms showing distributions of hydrocarbon fractions obtained from a typical sample of Core MD052911 (461 cm depth) (a) and a representative sample of Core ORI-860-22 (172 cm depth) (b). IS is internal standard and C_{23}–C_{33} denote *n*-alkanes comprised of 23–33 carbon atoms. Both records show the presence of C_{23}–C_{33} *n*-alkanes with odd carbon numbers, but PMI is only detected in one sample (b).

$$U_{37}^{K'} = C_{37:2}/\left(C_{37:2} + C_{37:3}\right), \quad (1)$$

$$SST = \left(U_{37}^{K'} - 0.044\right)/0.033. \quad (2)$$

3.2 *MOA biomarkers*

PMI is a diagnostic biomarker of MOA, and it was detected in only one sample (172 cm depth) in Core ORI-860-22 (Fig. 2b). The TOC normalized PMI content is 308 ng/g and the $\delta^{13}C$ value (–123‰) is much more negative compared with those of *n*-alkanes (–32.8‰ to –22.3‰) in the sample. However, another MOA biomarker (crocetane) was below the detection limit in this sample.

Diagnostic biomarkers of MOA in the neutral fractions were also only detected in one sample of ORI-860-22 (Fig. 4b). At 172 cm depth, the TOC normalized content was 8 491 ng/g for archaeol and 182 ng/g for *sn*-2-hydroxyarchaeol, respectively. In the same sample, TOC normalized content of dinosterol reached a maximum (1 220 ng/g), whereas brassicaterol content was lower (150 ng/g), and alkenones were below the detection limit.

3.3 *iso-GDGTs*

GDGT-0 to GDGT-3, Crenarchaeol and its regio-isomer were detected in all samples (Fig. 5). The TOC normalized content of total *iso*-GDGTs (GDGT-0 to 3, Crenarchaeol and Cre_isomer) was also plotted in Fig. 3, which revealed a broadly similar trend with those of the phytoplankton biomarkers in Core MD052911 (Fig. 3a), but a noticeably different trend from those of the phytoplankton biomarkers in Core ORI-860-22 (Fig. 3b). The TOC normalized *iso*-GDGTs content in Core MD052911 varied from 1 296 to 5 463 ng/g with an average of 3 527 ng/g. In Core ORI-860-22, there was an abnormal higher value (33 319 ng/g) for *iso*-GDGTs at 172 cm depth, but the *iso*-GDGTs content for the other samples varied in the range of 1 843–4 254 ng/g with an average of 2 881 ng/g.

TEX_{86} temperatures were calculated using the global core-top equation (Eq. (3)) (Schouten et al., 2002; Kim et al., 2008). TEX_{86} temperatures varied from 19.7°C to 29.3°C with an average of 23.4°C in Core MD052911, and from 10°C to 22.6°C with an average of 20.4°C (except the abnormal sample at 172 cm depth) in Core ORI-860-22.

$$TEX_{86} = \frac{[GDGT-2]+[GDGT-3]+[Cre-isomer]}{[GDGT-1]+[GDGT-2]+[GDGT-3]+[Cre-isomer]}$$
$$SST = 56.2 \times TEX_{86} - 10.78. \quad (3)$$

4 Discussion

4.1 *Terrestrial and marine organic matter contributions*

Lipids in our records are dominated by a mixture of biomarkers, including *n*-alkanes with an odd-over-even predominance derived from terrestrial higher plants and brassicasterol, dinosterol and alkenones derived from marine phytoplankton (diatoms, dinoflagellates and haptophytes) (Boon et al., 1979; Marlowe et al., 1984; Volkman et al., 1998; Zhao et al., 2003). Recently, biomarker ratios have been increasingly used as proxies to distinguish sedimentary organic matter sources and to estimate the relative contributions of terrestrial and marine organic matter (referred as TOM and MOM, respectively). $P_{mar\text{-}aq}$, $[C_{23}+C_{25}]/[C_{23}+C_{25}+C_{29}+C_{31}]$, was designed to be applied for coastal sedimentary organic matter source assessments, with low values (0.01–0.25) indicative of OM dominantly from terrestrial inputs, medium values (0.4–0.6) from emergent aquatic plants including mangroves and high values (>0.6) from aquatic plants and marine macrophytes (Sikes et al., 2009). The TMBR (terrestrial and marine biomarker ratio, Eq. (4)) index is based on the

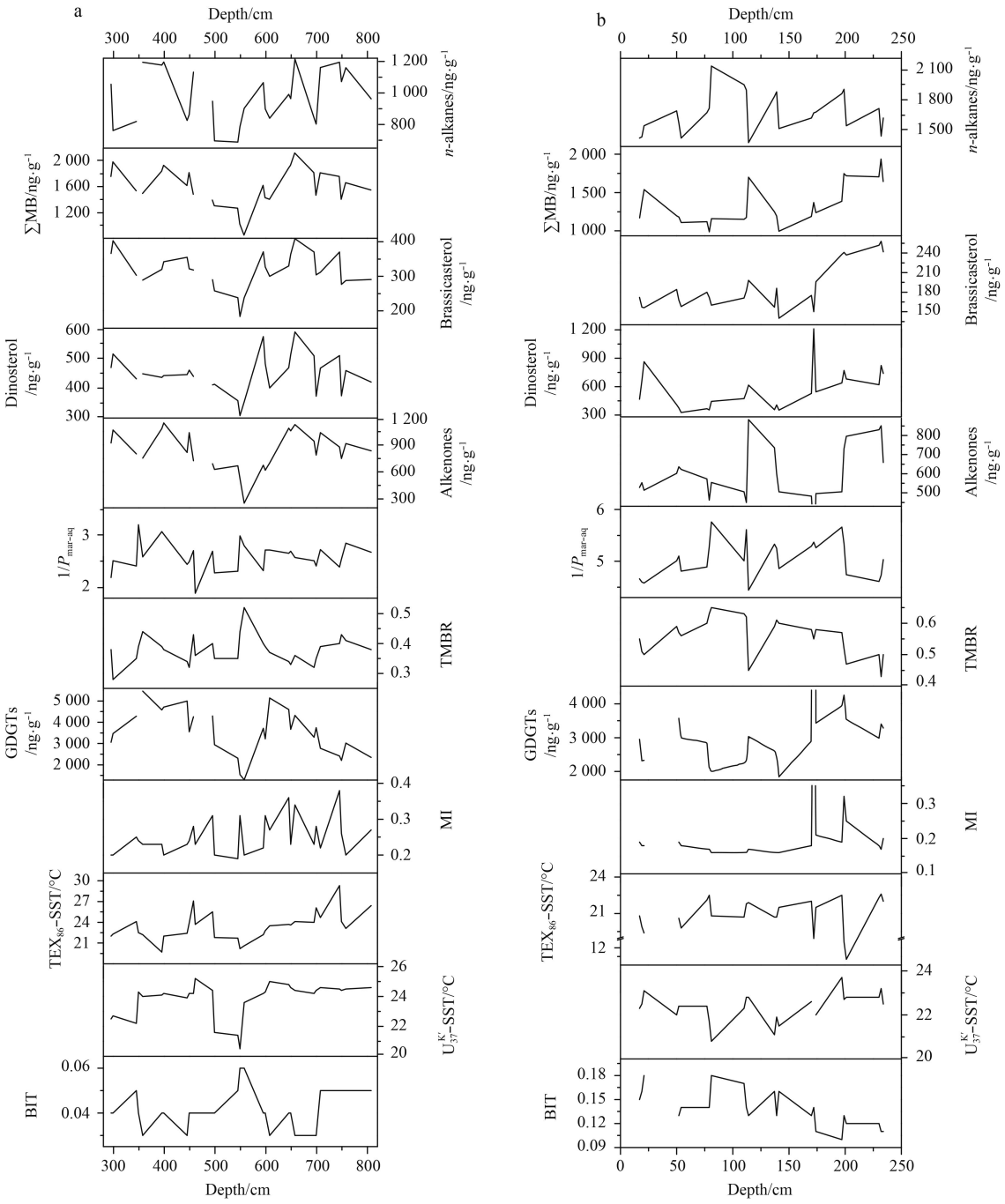

Fig. 3. Depth profiles of TOC normalized content (ng/g) of *n*-alkanes, brassicasterol, dinosterol, alkenones and *iso*-GDGTs, and organic geochemical indexes ($1/P_{mar\text{-}aq}$, TMBR, MI, SST, BIT) for Core MD052911 (a) and Core ORI-860-22 (b). a. For Core MD052911, two samples at 349 cm and 461 cm depth were not analyzed for TOC due to the lack of sufficient samples; and b. for Core ORI-860-22, GDGTs were not determined in one sample located at 50 cm due to the loss of the fraction, and alkenones were not detected in a sample at 172 cm depth. Detailed sample information and origin data can be found in Table A1 and Table A2.

ratio between *n*-alkanes (C_{27}+C_{29}+C_{31}) and phytoplankton biomarkers (brassicasterol, dinosterol and C_{37} alkenones, referred as B+D+A), and used to estimate the relative TOM contribution (Xing et al., 2014). We use $1/P_{mar\text{-}aq}$ to compare with TMBR and focus on estimating terrestrial OM inputs, with higher value (>4) indicating TOM domination and lower value (<1.7) indicating dominant contribution from aquatic and marine sources (Xing et al., 2011). One advantage of using these ratio-based proxies is that even though biomarker contents were significantly affected by biodegradation, sedimentary biomarker ratios were not significantly affected (Versteegh and Zonneveld, 2002).

$$TMBR = \frac{(C_{27} + C_{29} + C_{31}n\text{–alkanes})}{(C_{27} + C_{29} + C_{31}n\text{–alkanes}) + (B + D + A)}. \quad (4)$$

Using *n*-alkanes and ∑MB as proxies for TOM and MOM contents, then lower average *n*-alkanes content in Core MD052911 (971 ng/g) than that in Core ORI-860-22 (1 674 ng/g) suggested

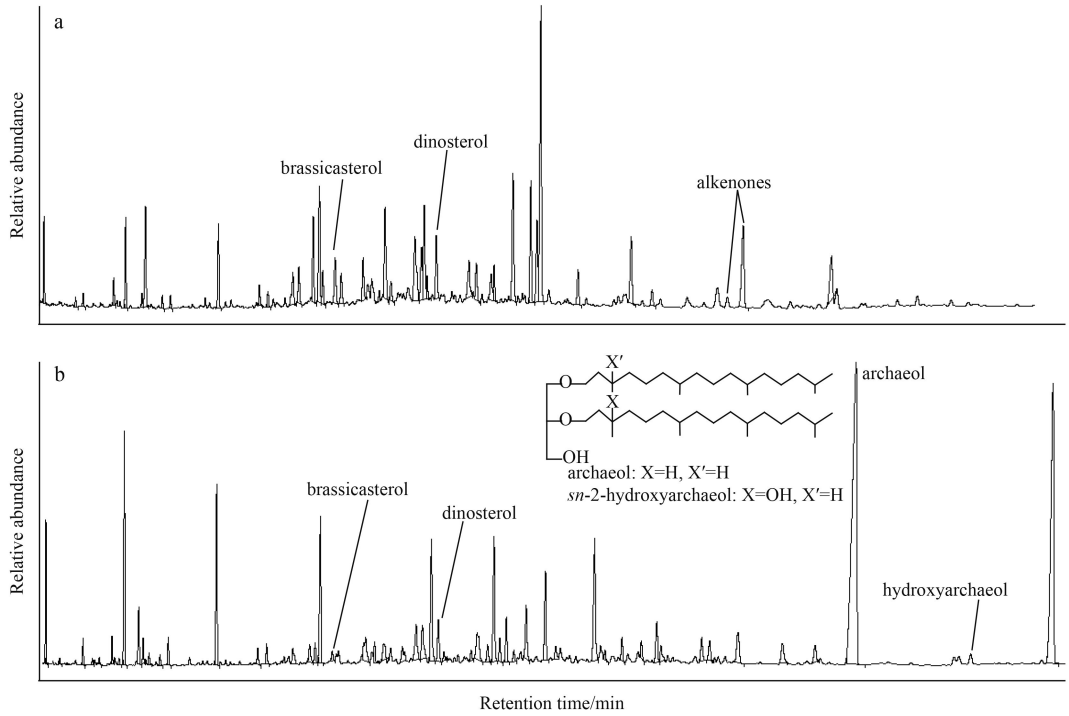

Fig. 4. Partial gas chromatograms of derivatives of neutral lipids in Core MD052911 (461 cm depth) (a) and Core ORI-860-22 (172 cm depth) (b), including sterols, alkenones and MOA biomarkers. Brassicasterol and dinosterol were shown in all records, but archaeol and hydroxyarchaeol were only detected in Fig. b and C_{37}-alkenones were not detected.

lower TOM inputs in Core MD052911 (Figs 3a and b); and average ∑MB values in the two cores suggested slightly higher MOM inputs in MD052911 than that in Core ORI-860-22 (Figs 3a and b). Qualitatively, biomarker contents suggested that marine inputs were the dominant sources for organic matter in MD052911 sediments, while both terrestrial and marine inputs contributed to the total organic matter in ORI-860-22 sediments. The TMBR and $1/P_{\text{mar-aq}}$ indexes both revealed lower average values in Core MD052911 (0.38 and 2.6, respectively) relative to those in Core ORI-860-22 (0.56 and 5.05, respectively), which quantitatively indicated that MOM dominated OM sources in Core MD052911 and Core ORI-860-22 OM was mainly derived from terrestrial inputs. Both cores were retrieved from the Kaoping Slope off SW Taiwan with a high flux of terrigenous suspended sediments exported from the adjacent rivers with particle load of 104 Mt/a for today (Dadson et al., 2003), contributing the relatively high TOM contribution in both cores. Core ORI-860-22 is located south of Core MD052911 with a deeper water depth, it is inferred that different morphologies were the likely reason for the TOM percentage, with Core MD052911 locating at anticlinal strata and resulting in lower TOM percentage.

GDGTs results provide additional evidence for estimates of TOM and MOM contributions in these cores. *iso*-GDGTs biosynthesized by marine *Crenarchaeota* and a large number of membrane-metabolizing archaea are ubiquitous in marine environments (Sinninghe Damsté et al., 2002a, b; Schouten et al., 2013), and can be used as MOM indicators. TOC normalized content of *iso*-GDGTs in Core MD052911 is obviously higher than that in Core ORI-860-22 (excluding the abnormally high point), which is consistent with the higher MOM contributions in Core MD052911 estimated by ∑MB. Similar variations between *iso*-GDGTs and marine biomarkers (sterols and alkenones) in Core MD052911 suggested that these ether-bound lipids are derived from the archaea utilizing a carbon source unaffected by the oxidation of methane (Schouten et al., 2013). Whereas, different trends between *iso*-GDGTs and marine biomarkers in Core ORI-860-22 would indicate other sources for *iso*-GDGTs, such as from methane oxidation microbes (Blumenberg et al., 2004; Weijers et al., 2011; Zhang et al., 2011; Schouten et al., 2013). Quantitative estimates of TOM contribution can also be made using the BIT index, based on the ratio of Crenarchaeol and branched-GDGT compounds (referred as GDGT-I/-II/-III in Fig. 5c) (Eq. (5)) (Hopmans et al., 2004). Samples from open ocean settings contain very low amounts of brGDGTs, which resulted in low BIT values ranging from 0.01 to 0.08; and maximum BIT values of 0.98-1 are found for the samples of terrestrial origin, i.e., no aquatic input (Hopmans et al., 2004). BIT values in Core MD052911 samples ranged from 0.03 to 0.06 (0.04 on average), while BIT values ranged from 0.1 to 0.18 (0.14 on average) in Core ORI-860-22 samples. Lower TOM contribution in Core MD052911 indicated by the BIT index is consistent with TMBR estimates; but for quantitative estimates, BIT values indicated relatively low TOM percentage in comparison with TMBR estimates in both cores, probably due to the underestimate of TOM contribution by BIT index (Weijers et al., 2009). One reason for the difference is that BIT index only reflects soil OM input but TMBR represents both soil and plant OM input (Xing et al., 2014), because brGDGTs are only derived from anaerobic soil bacteria and transported to the coastal regions mainly by fluvial processes, while *n*-alkanes can be delivered by both rivers and aeolian dusts (Weijers et al., 2009; Xing et al., 2011, 2014; Smith et al., 2012; Schouten et al., 2013). Thus, the BIT results would suggest that river-transported terrestrial soil OM was not a major source of TOM of sedimentary OM around these settings, but a slightly higher contribution in Core ORI-860-22 than that in Core MD052911. On the other hand, degradation of brGDGTs during

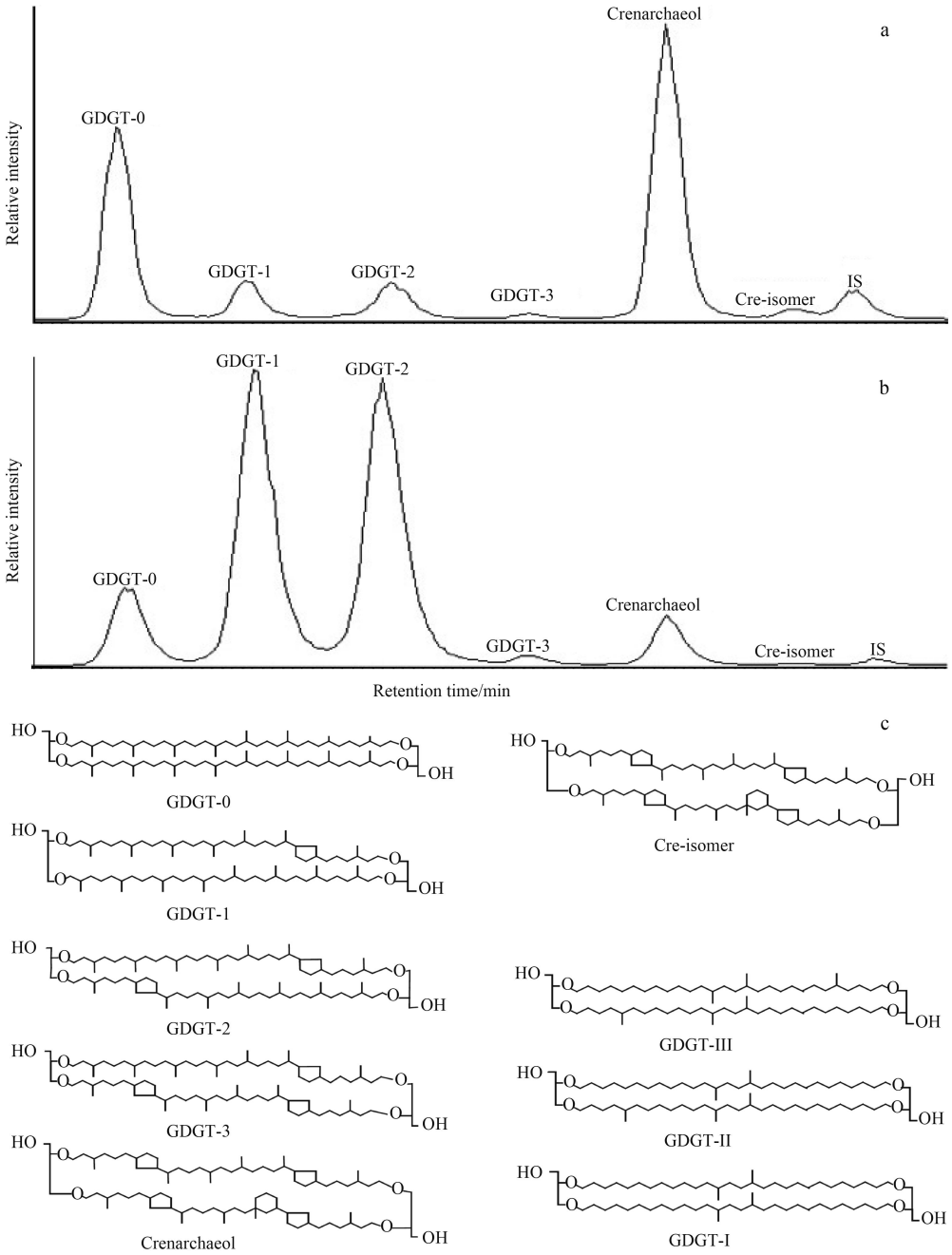

Fig. 5. HPLC-MS total ion current traces of *iso*-GDGTs in two sediments of Core MD052911 (a) and Core ORI-860-22 (b) from the Kaoping Slope. GDGT-0 to GDGT-3 refers to the number of cyclopetane moieties (0–3) of the *iso*-GDGTs, with structures sketched in the bottom panel (c).

transport processes could also result in an underestimate of TOM contribution using the BIT index. The distributions of brGDGTs in sediments from the lower Changjiang River and East China Sea shelf indicated that ca. 95% of brGDGTs were degraded in the estuary region and the BIT proxy do not reflect the catchment environmental conditions (Zhu et al., 2011). Xing et al. (2014) also found that brGDGTs were deposited near estuaries and coasts had a lower content offshore, while a significant portion of *n*-alkanes could be deposited further offshore.

$$BIT=\frac{[\text{GDGT–I}]+[\text{GDGT–II}]+[\text{GDGT–III}]}{[\text{GDGT–I}]+[\text{GDGT–II}]+[\text{GDGT–III}]+[\text{Crenarchaeol}]} \quad (5)$$

4.2 *Comparison of biomarker characteristics in normal and AOM-influenced sediments*

In Core ORI-860-22, three diagnostic MOA biomarkers (PMI, archaeol and hydroxyarchaeol) were present at relatively high concentrations for the sample at 172 cm, but these biomarkers were not detected in other analyzed samples. In addition, the δ^{13}C value of PMI (–123‰) was much more negative compared with the δ^{13}C values of *n*-alkanes (–22.3‰ to –32.8‰) from marine algae and terrestrial higher plants in the same sample. The co-occurrence of PMI, archaeol and hydroxyarchaeol with more depleted δ^{13}C values is typical for many AOM settings (Elvert et al., 1999; Pancost et al., 2001; Pancost and Damste, 2003; Elvert et al., 2005; Pape et al., 2005; Guan et al., 2013). Therefore, our res-

ults could indicate significant AOM activities at or around 172 cm depth of Core ORI-860-22. However in Core MD052911, archaeal biomarkers were not detected in any of the analyzed sediment samples, suggesting absence of AOM activities. Previous studies of four sediment samples from the Dongsha Islands area of the South China Sea revealed that archaeal biomarkers PMI and crocetane only occurred below the sulfate-methane transition zone (SMTZ) with maximum concentrations close to the SMTZ (Yu et al., 2008). On the Northern European continental margin, archaeol concentration typically reached maximum values close to the SMTZ with decreasing concentration below the SMTZ at all studied sites, but was below detection limit in shallower sediments at most sites (Aquilina et al., 2010); hydroxyarchaeal and PMI were only present at and below the SMTZ at most sites (Aquilina et al., 2010). However, crocetane, another MOA biomarker, was not detected in any sediment samples in their study of brackish-marine sediments offshore Northern Europe (Aquilina et al., 2010). It has been suggested that the concentration of specific MOA biomarkers is influenced by the amount of upward transport of methane (Lee et al., 2013), our results thus indicated that the upward methane seepage was not continuous or the flux of methane was not sufficient to induce high AOM activities in our locations, resulting in below-detection concentrations of MOA biomarkers in Core MD052911 samples and most samples of Core ORI-860-22. On the other hand, the presence of high concentrations of allochthonous OM could obscure the detection of MOA biomarkers (Aquilina et al., 2010). TOM was an important component of sedimentary OM in both cores, but MOA biomarkers were detected in Core ORI-860-22 even though its TOM percentage was higher. As a result, TOM effect was not likely the main reason for the absence of MOA biomarkers in these sediment samples.

GDGTs based proxies can also be used to evaluate the influences of AOM on our samples. Previous research has indicated that AOM in a variety of settings can influence sedimentary iso-GDGT distributions, by producing a higher proportion of GDGT-1 and GDGT-2 (Weijers et al., 2011; Zhang et al., 2011). The different distributions of *iso*-GDGTs in Cores MD052911 and ORI-860-22 (Fig. 3) could indicate the AOM effects, specifically at 172 cm depth in Core ORI-860-22 where *iso*-GDGTs contents reached abnormal maximum value and dominated by GDGT-1 and GDGT-2 (Figs 3b and 5b). TEX_{86} temperature differences between the cores also likely reflected the effects of AOM. TEX_{86} temperatures calculated using the global core-top equation in Core ORI-860-22 (10–22.6°C, average 20.4°C) were significantly lower than those in Core MD052911 (19.7–29.3°C, average 23.4°C); in addition, TEX_{86} temperatures were lower than the $U^{K'}_{37}$ temperatures (20.8–23.7°C, average 22.8°C) in Core ORI-860-22, while TEX_{86} temperatures were similar to $U^{K'}_{37}$ temperatures (20.5–25°C, average 23.8°C) in Core MD052911. One possible reason for lower TEX_{86} temperatures is the influence of terrestrial *iso*-GDGTs, which can be evaluated by comparing the BIT index. As discussed above, BIT values in all samples were below 0.2, indicating that river input of terrestrial *iso*-GDGTs could not bias the TEX_{86} proxy (Weijers et al., 2006) in our samples. The more likely reason is the additional contributions to sedimentary *iso*-GDGTs from AOM activities, as previous studies have suggested that at high AOM activity sites, the application of TEX_{86} was restricted due to the additional methanogens contribution to *iso*-GDGTs, and *iso*-GDGTs distribution pattern could no longer be explained by temperature-induced physiological responses (Schouten et al., 2002; Zhang et al., 2011). Thus, the different patterns of TEX_{86} and $U^{K'}_{37}$ temperatures in these two sediment cores could indicate that AOM affected TEX_{86} temperature estimates in Core ORI-860-22, but not significantly on TEX_{86} temperature estimates in Core MD052911. This result is consistent with a previous study using samples from the hydrate-rich region in the Qiongdongnan Basin of the northern South China Sea, which also concluded that the lipids in the sediments were predominantly from planktonic archaea and the TEX_{86}-derived temperatures were unlikely to be biased by AOM activity due to the lower abundances of *iso*-GDGTs from methane-metabolizing archaea (Wei et al., 2014).

The Methane Index (MI), consisting of the relative distribution of *iso*-GDGTs (Eq. (6)), has been proposed to distinguish gas hydrate impacted and/or methane-rich deep sea environments from normal marine realm (Zhang et al., 2011). MI values range from 0 to 1, and 0.3 is proposed to mark the boundary between hydrate-impacted sediments and normal marine sediments. Higher MI values could indicate strong impact of AOM microbial communities, whereas low values characterize normal marine sedimentary conditions (Zhang et al., 2011).

$$MI = \frac{[\mathrm{GDGT\text{–}1}] + [\mathrm{GDGT\text{–}2}] + [\mathrm{GDGT\text{–}3}]}{[\mathrm{GDGT\text{–}1}] + [\mathrm{GDGT\text{–}2}] + [\mathrm{GDGT\text{–}3}] + [\mathrm{Crenarchaeol}] + [\mathrm{Cre\text{–}isomer}]}\ ,$$
$$(0 \leqslant MI \leqslant 1)\,. \tag{6}$$

There were clear differences in MI values between normal sediments and the sediment containing MOA biomarkers in our samples (Fig. 3). In Core ORI-860-22, the maximum MI value of 0.94 at 172 cm depth, dominated by GDGT-1 and GDGT-2. According to previous research, MI values close to 1 clearly showed significant contributions of methanotrophic archaeal community to sediment *iso*-GDGTs (Zhang et al., 2011), thus maximum MI value at 172 cm depth would indicate high AOM activities and be consistent with the detection of the three diagnostic MOA biomarkers (PMI, archaeol and hydroxyarchaeol). MI values for the other samples in Core ORI-860-22 ranged from 0.16 to 0.32 with most values lower than or around 0.3, indicating insignificant contribution of MOA *iso*-GDGTs and consistent with the absence of MOA lipid biomarkers in these samples. In Core MD052911, MI values ranged between 0.19 and 0.38, indicating insignificant contributions of *iso*-GDGTs from methanotrophic archaea, which is also consistent with MOA lipid biomarker results. However, the average MI value in Core MD052911 (0.25) is slightly higher than that in Core ORI-860-22 (0.19, excluding the value for 172 cm sample), and this is likely related to the temperature effect on MI. A previous study using 426 surface sediment samples indicated that MI values increase with increasing TEX_{86} SSTs (Zhang et al., 2011), and this is likely caused by the slight SST dependence of MI values in planktonic *Crenarchaeota*, without involving methanotrophic *Euryarchaeota* (Zhang et al., 2011). Thus, in our results, both MI values and TEX_{86} SSTs were higher in Core MD052911 than those in Core ORI-860-22.

5 Conclusions

Two piston cores retrieved from potential cold seep areas of

the South China Sea off SW Taiwan were analyzed using organic geochemical approach. TOC normalized contents of terrestrial and marine biomarkers qualitatively suggest that marine inputs were the dominant sources for organic matter in MD052911 sediments, while both terrestrial and marine inputs contributed to the total organic matter in ORI-860-22 sediments. TOC normalized content of *iso*-GDGTs and biomarker ratio proxies further indicated that MOM dominated OM sources in Core MD052911 and OM in Core ORI-860-22 was mainly derived from terrestrial inputs, and different morphologies were the likely reason for the differences.

MOA diagnostic biomarkers (PMI, archaeol and hydroxyarchaeol) were only detected in one sample at 172 cm depth of Core ORI-860-22. With co-occurrence of abnormal maximum *iso*-GDGTs content and MI value (0.94), these results could indicate significant AOM activities at or around 172 cm. However in Core MD052911, MOA biomarkers were not detected in any of the samples and MI values were lower (0.19–0.38), suggesting absence of AOM activities and insignificant contributions of *iso*-GDGTs from methanotrophic archaea. The different distributions of *iso*-GDGTs in two cores could also indicate the AOM effects, with the dominance of GDGT-1 and GDGT-2 in Core ORI-860-22. Biomarker results thus indicated that the upward methane seepage was not continuous or the flux of methane was not sufficient to induce high AOM activities in our sampling sites.

TEX_{86} temperatures were lower than $U^{K'}_{37}$ temperatures in Core ORI-860-22, while those temperatures were similar in Core MD052911. The different patterns of TEX_{86} and $U^{K'}_{37}$ temperature in two cores could indicate that AOM activities influence TEX_{86} temperature estimates with lower values in Core ORI-860-22, but not significantly on TEX_{86} temperature estimates in Core MD052911.

Acknowledgements

The authors thank Zhang Hailong for technical help, Yang Tsanyao Frank for useful discussion. We thank reviewers for constructive comments. This is the Key Laboratory of Marine Chemistry Theory and Technology (MCTL) contribution #113.

References

Aquilina A, Knab N J, Knittel K, et al. 2010. Biomarker indicators for anaerobic oxidizers of methane in brackish-marine sediments with diffusive methane fluxes. Org Geochem, 41(4): 414–426

Bian Liangqiao, Hinrichs K U, Xie Tianmin, et al. 2001. Algal and archaeal polyisoprenoids in a recent marine sediment: molecular isotopic evidence for anaerobic oxidation of methane. Geochem Geophys Geosyst, 2(1): doi: 10.1029/2000GC000112

Biddle J F, Lipp J S, Lever M A, et al. 2006. Heterotrophic Archaea dominate sedimentary subsurface ecosystems off Peru. Proc Natl Acad Sci U S A, 103(10): 3846–3851

Blumenberg M, Seifert R, Reitner J, et al. 2004. Membrane lipid patterns typify distinct anaerobic methanotrophic consortia. Proc Natl Acad Sci U S A, 101(30): 11111–11116

Boetius A, Ravenschlag K, Schubert C J, et al. 2000. A marine microbial consortium apparently mediating anaerobic oxidation of methane. Nature, 407(6804): 623–626

Boon J J, Rijpstra W I C, de Lange F, et al. 1979. Black sea sterol—a molecular fossil for dinoflagellate blooms. Nature, 277(5692): 125–127

Bouloubassi I, Aloisi G, Pancost R D, et al. 2006. Archaeal and bacterial lipids in authigenic carbonate crusts from eastern Mediterranean mud volcanoes. Org Geochem, 37(4): 484–500

Chen Zhong, Huang C Y, Zhao Meixun, et al. 2011. Characteristics and possible origin of native aluminum in cold seep sediments from the northeastern South China Sea. J Asian Earth Sci, 40(1): 363–370

Chi W C, Reed D L, Liu C S, et al. 1998. Distribution of the bottom-simulating reflector in the offshore Taiwan collision zone. Terrestr Atmos Ocean Sci, 9(4): 779–794

Chuang P C, Yang T F, Lin S, et al. 2006. Extremely high methane concentration in bottom water and cored sediments from offshore southwestern Taiwan. Terrestr Atmos Ocean Sci, 17(4): 903–920

Dadson S J, Hovius N, Chen H, et al. 2003. Links between erosion, runoff variability and seismicity in the Taiwan orogen. Nature, 426(6967): 648–651

Elvert M, Hopmans E C, Treude T, et al. 2005. Spatial variations of methanotrophic consortia at cold methane seeps: implications from a high-resolution molecular and isotopic approach. Geobiology, 3(3): 195–209

Elvert M, Suess E, Whiticar M J. 1999. Anaerobic methane oxidation associated with marine gas hydrates: superlight C-isotopes from saturated and unsaturated C_{20} and C_{25} irregular isoprenoids. Naturwissenschaften, 86(6): 295–300

Guan Hongxiang, Sun Yongge, Zhu Xiaowei, et al. 2013. Factors controlling the types of microbial consortia in cold-seep environments: a molecular and isotopic investigation of authigenic carbonates from the South China Sea. Chem Geol, 354: 55–64

Hinrichs K U, Summons R E, Orphan V, et al. 2000. Molecular and isotopic analysis of anaerobic methane-oxidizing communities in marine sediments. Org Geochem, 31(12): 1685–1701

Hoehler T M, Alperin M J, Albert D B, et al. 1994. Field and laboratory studies of methane oxidation in an anoxic marine sediment: evidence for a methanogen-sulfate reducer consortium. Global Biogeochem Cycles, 8(4): 451–463

Hopmans E C, Schouten S, Pancost R D, et al. 2000. Analysis of intact tetraether lipids in archaeal cell material and sediments by high performance liquid chromatography/atmospheric pressure chemical ionization mass spectrometry. Rapid Commun Mass Spectrom, 14(7): 585–589

Hopmans E C, Weijers J W H, Schefuß E, et al. 2004. A novel proxy for terrestrial organic matter in sediments based on branched and isoprenoid tetraether lipids. Earth Planet Sci Lett, 224(1–2): 107–116

Huang C Y, Chien C W, Zhao Meixun, et al. 2006a. Geological investigations of active cold seeps in the syn-collision accretionary prism Kaoping slope off SW Taiwan. Terrestr Atmos Ocean Sci, 17(4): 679–702

Huang C Y, Yuan P B, Tsao S J. 2006b. Temporal and spatial records of active arc-continent collision in Taiwan: a synthesis. Geological Society of America Bulletin, 118(3–4): 274–288

Kaneko M, Naraoka H, Takano Y, et al. 2013. Distribution and isotopic signatures of archaeal lipid biomarkers associated with gas hydrate occurrences on the northern Cascadia Margin. Chem Geol, 343: 76–84

Kim J H, Schouten S, Hopmans E C, et al. 2008. Global sediment core-top calibration of the TEX_{86} paleothermometer in the ocean. Geoch Cosmochim Acta, 72(4): 1154–1173

Lee D H, Kim J H, Bahk J J, et al. 2013. Geochemical signature related to lipid biomarkers of ANMEs in gas hydrate-bearing sediments in the Ulleung Basin, East Sea (Korea). Mar Pet Geol, 47: 125–135

Lin S, Hsieh W C, Lim Y C, et al. 2006. Methane migration and its influence on sulfate reduction in the Good Weather Ridge region, South China Sea continental margin sediments. Terrestr Atmos Ocean Sci, 17(4): 883–902

Liu C S, Deffontaines B, Lu C Y, et al. 2004. Deformation patterns of an accretionary wedge in the transition zone from subduction to collision offshore southwestern Taiwan. Mar Geophys Res, 25(1–2): 123–137

Liu C S, Schnürle P, Wang Y S, et al. 2006. Distribution and characters of gas hydrate offshore of southwestern Taiwan. Terrestr Atmos Ocean Sci, 17(4): 615–644

Marlowe I T, Brassell S C, Eglinton G, et al. 1984. Long chain unsaturated ketones and esters in living algae and marine sediments. Org Geochem, 6: 135–141

Müller P J, Kirst G, Ruhland G, et al. 1998. Calibration of the alken-

one paleotemperature index $U_{37}^{K'}$ based on core-tops from the eastern South Atlantic and the global ocean (60°N–60°S). Geochim Cosmochim Acta, 62(10): 1757–1772

Orphan V J, Hinrichs K U, Ussler W III, et al. 2001. Comparative analysis of methane-oxidizing archaea and sulfate-reducing bacteria in anoxic marine sediments. Appl Environ Microbiol, 67(4): 1922–1934

Pancost R D, Damste J S S. 2003. Carbon isotopic compositions of prokaryotic lipids as tracers of carbon cycling in diverse settings. Chem Geol, 195(1–4): 29–58

Pancost R D, Hopmans E C, Damsté J S S. 2001. Archaeal lipids in Mediterranean cold seeps: molecular proxies for anaerobic methane oxidation. Geochim Cosmochim Acta, 65(10): 1611–1627

Pape T, Blumenberg M, Seifert R, et al. 2005. Lipid geochemistry of methane-seep-related Black Sea carbonates. Palaeogeogr Palaeoclimatol Palaeoecol, 227(1–3): 31–47

Parkes R J, Cragg B A, Banning N, et al. 2007. Biogeochemistry and biodiversity of methane cycling in subsurface marine sediments (Skagerrak, Denmark). Environ Microbiol, 9(5): 1146–1161

Reeburgh W S, Ward B B, Whalen S C, et al. 1991. Black Sea methane geochemistry. Deep Sea Res Part A: Oceanogr Res Papers, 38(S2): S1189–S1210

Reeburgh W S. 2007. Oceanic methane biogeochemistry. Chem Rev, 107(2): 486–513

Schouten S, Hopmans E C, Schefuß E, et al. 2002. Distributional variations in marine crenarchaeotal membrane lipids: a new tool for reconstructing ancient sea water temperatures?. Earth Planet Sci Lett, 204(1–2): 265–274

Schouten S, Hopmans E C, Sinninghe Damsté J S. 2013. The organic geochemistry of glycerol dialkyl glycerol tetraether lipids: a review. Org Geochem, 54: 19–61

Sikes E L, Uhle M E, Nodder S D, et al. 2009. Sources of organic matter in a coastal marine environment: evidence from *n*-alkanes and their δ^{13}C distributions in the Hauraki Gulf, New Zealand. Mar Chem, 113(3–4): 149–163

Sinninghe Damsté J S, Rijpstra W I C, Hopmans E C, et al. 2002a. Distribution of membrane lipids of planktonic *Crenarchaeota* in the Arabian Sea. Appl Environ Microbiol, 68(6): 2997–3002

Sinninghe Damsté J S, Schouten S, Hopmans E C, et al. 2002b. Crenarchaeol: the characteristic core glycerol dibiphytanyl glycerol tetraether membrane lipid of cosmopolitan pelagic crenarchaeota. J Lipid Res, 43(10): 1641–1651

Smith R W, Bianchi T S, Li Xinxin. 2012. A re-evaluation of the use of branched GDGTs as terrestrial biomarkers: implications for the BIT Index. Geochim Cosmochim Acta, 80: 14–29

Stadnitskaia A, Bouloubassi I, Elvert M, et al. 2008. Extended hydroxyarchaeol, a novel lipid biomarker for anaerobic methanotrophy in cold seepage habitats. Org Geochem, 39(8): 1007–1014

Versteegh G J M, Zonneveld K A F. 2002. Use of selective degradation to separate preservation from productivity. Geology, 30(7): 615–618

Volkman J K, Barrett S M, Blackburn S I, et al. 1998. Microalgal biomarkers: a review of recent research developments. Org Geochem, 29(5–7): 1163–1179

Wegener G, Boetius A. 2009. An experimental study on short-term changes in the anaerobic oxidation of methane in response to varying methane and sulfate fluxes. Biogeosciences, 6(5): 867–876

Wei Yuli, Wang Peng, Zhao Meixun, et al. 2014. Lipid and DNA evidence of dominance of planktonic archaea preserved in sediments of the South China Sea: insight for application of the TEX_{86} proxy in an unstable marine sediment environment. Geomicrobiol J, 31(4): 360–369

Weijers J W H, Lim K L H, Aquilina A, et al. 2011. Biogeochemical controls on glycerol dialkyl glycerol tetraether lipid distributions in sediments characterized by diffusive methane flux. Geochem Geophys Geosyst, 12(10): Q10010

Weijers J W H, Schouten S, Schefuß E, et al. 2009. Disentangling marine, soil and plant organic carbon contributions to continental margin sediments: a multi-proxy approach in a 20,000 year sediment record from the Congo deep-sea fan. Geochim Cosmochim Acta, 73(1): 119–132

Weijers J W H, Schouten S, Spaargaren O C, et al. 2006. Occurrence and distribution of tetraether membrane lipids in soils: implications for the use of the TEX_{86} proxy and the BIT index. Org Geochem, 37(12): 1680–1693

Xing Lei, Zhang Hailong, Yuan Zineng, et al. 2011. Terrestrial and marine biomarker estimates of organic matter sources and distributions in surface sediments from the East China Sea shelf. Cont Shelf Res, 31(10): 1106–1115

Xing Lei, Zhao Meixun, Gao Wenxian, et al. 2014. Multiple proxy estimates of source and spatial variation in organic matter in surface sediments from the southern Yellow Sea. Org Geochem, 76: 72–81

Yu Xiaoguo, Han Xiqiu, Li Hongliang, et al. 2008. Biomarkers and carbon isotope composition of anaerobic oxidation of methane in sediments and carbonates of northeastern part of Dongsha, South China Sea. Haiyang Xuebao (in Chinese), 30(3): 77–84

Zhang C L, Li Yiliang, Wall J D, et al. 2002. Lipid and carbon isotopic evidence of methane-oxidizing and sulfate-reducing bacteria in association with gas hydrates from the Gulf of Mexico. Geology, 30(3): 239–242

Zhang Yige, Zhang Chuanlun, Liu Xiaolei, et al. 2011. Methane Index: a tetraether archaeal lipid biomarker indicator for detecting the instability of marine gas hydrates. Earth Planet Sci Lett, 307(3–4): 525–534

Zhao Meixun, Dupont L, Eglinton G, et al. 2003. *n*-Alkane and pollen reconstruction of terrestrial climate and vegetation for N.W. Africa over the last 160 kyr. Org Geochemis, 34(1): 131–143

Zhu Chun, Weijers J W H, Wagner T, et al. 2011. Sources and distributions of tetraether lipids in surface sediments across a large river-dominated continental margin. Org Geochem, 42(4): 376–386

Appendix:

Table A1. Sample information; TOC; contents of odd *n*-alkanes (C_{27}+C_{29}+C_{31} *n*-alkanes) and marine phytoplankton biomarkers (brassicasterol, dinosterol, C_{37} alkenones) (ng/g); contents of total *iso*-GDGTs (GDGT-0 to -3, Crenarcheol and Cre-isomer) (ng/g); $U^{K'}_{37}$-SST and TEX_{86}-SST (°C); and $1/P_{mar\text{-}aq}$, TMBR, BIT, MI indexes

Core	Longitude	Latitude	Depth/cm	TOC/%	Odd *n*-alkanes/ ng·g^{-1}	Brassicasterol/ ng·g^{-1}	Dinosterol/ ng·g^{-1}	Alkenones/ ng·g^{-1}	*iso*-GDGTs/ ng·g^{-1}	$U^{K'}_{37}$-SST/°C	TEX_{86}-SST/°C	$1/P_{mar\text{-}aq}$	TMBR	BIT	MI
MD052911	119°51.08′E	22°15.61′N	295	0.71	747	259	332	654	2 164	22.5	22.0	2.19	0.38	0.04	0.20
			299	0.69	524	277	353	734	2 385	22.7	22.3	2.51	0.28	0.04	0.20
			345	0.64	524	194	276	513	2 742	22.2	24.1	2.41	0.35	0.05	0.25
			349	n.d.	997	239	336	964	2 847	24.3	22.5	3.19	0.39	0.04	0.24
			357.5	0.74	880	213	330	557	4 026	24.0	22.2	2.58	0.44	0.03	0.23
			395	0.73	853	232	316	786	3 324	24.1	19.7	3.06	0.39	0.04	0.23
			399	0.70	834	238	308	800	3 285	24.2	22.0	3.01	0.38	0.04	0.20
			445	0.66	549	236	296	542	3 322	23.9	22.4	2.44	0.34	0.03	0.23
			449	0.69	597	223	319	718	2 462	24.2	23.9	2.49	0.32	0.04	0.24
			457.5	0.61	693	195	268	444	2 603	24.2	27.1	2.70	0.43	0.04	0.28
			461	n.d.	698	249	297	692	2 989	25.2	23.7	1.89	0.36	0.04	0.23
			495	0.75	712	218	309	519	3 228	24.4	25.5	2.69	0.40	0.04	0.31
			499	0.73	511	189	303	461	2 163	21.6	21.8	2.28	0.35	0.04	0.20
			545	0.63	432	149	225	421	1 453	21.4	21.7	2.31	0.35	0.05	0.19
			549	0.62	487	114	191	325	953	20.5	20.2	2.98	0.44	0.06	0.31
			557.5	0.50	451	119	177	126	648	23.6	20.6	2.79	0.52	0.06	0.20
			595	0.56	595	208	320	378	2 078	24.2	22.2	2.32	0.40	0.04	0.22
			599	0.73	655	238	351	452	2 351	24.3	22.8	2.71	0.39	0.04	0.31
			607.5	0.73	609	218	291	508	3 728	25.0	23.5	2.71	0.37	0.03	0.27
			645	0.61	602	201	284	661	2 791	24.8	23.7	2.65	0.34	0.04	0.36
			649	0.63	603	228	320	661	2 295	24.6	23.6	2.69	0.33	0.04	0.23
			657.5	0.59	715	240	346	663	2 545	24.4	24.1	2.57	0.36	0.03	0.34
			695	0.61	515	226	311	577	2 017	24.2	24.0	2.51	0.32	0.03	0.23
			699	0.65	524	198	244	514	2 443	24.4	26.1	2.41	0.35	0.03	0.28
			707.5	0.64	745	200	300	665	1 781	24.6	24.7	2.72	0.39	0.05	0.22
			745	0.53	633	196	270	466	1 280	24.5	29.3	2.39	0.40	0.05	0.38
			749	0.68	724	188	253	507	1 491	24.4	24.1	2.54	0.43	0.05	0.26
			757.5	0.70	807	200	319	637	2 099	24.5	23.1	2.84	0.41	0.05	0.20
			807.5	0.62	599	182	261	520	1 464	24.6	26.4	2.67	0.38	0.05	0.27
ORI-860-22	119°50.63′E	22°13.08′N	17	0.47	671	81	220	248	1 383	22.3	20.8	4.66	0.55	0.15	0.19
			19	0.48	690	75	317	265	1 110	22.5	19.9	4.60	0.51	0.16	0.18
			21	0.48	745	75	418	247	1 120	23.1	19.4	4.58	0.50	0.18	0.18
			50	0.44	746	81	180	265	n.d.	22.0	n.d.	5.01	0.59	n.d.	n.d.
			52	0.53	830	89	198	334	1 880	22.4	20.6	5.10	0.57	0.13	0.19

to be continued

Continued from Table A1

Core	Longitude	Latitude	Depth/cm	TOC/%	Odd *n*-alkanes/ ng·g^{-1}	Brassicasterol/ ng·g^{-1}	Dinosterol/ ng·g^{-1}	Alkenones/ ng·g^{-1}	*iso*-GDGTs/ ng·g^{-1}	$U^{K'}_{37}$-SST/°C	TEX_{86}-SST/°C	$1/P_{mar\text{-}aq}$	TMBR	BIT	MI
			54	0.50	718	79	164	312	1 503	22.4	19.8	4.81	0.56	0.14	0.18
			77	0.48	807	87	176	276	1 374	22.4	22.1	4.89	0.60	0.14	0.17
			79	0.50	866	87	179	233	1 070	21.7	22.5	5.28	0.63	0.14	0.17
			81	0.45	963	72	201	251	907	20.8	20.8	5.76	0.65	0.18	0.16
			110	0.45	866	76	212	225	1 002	22.3	20.7	5.01	0.63	0.17	0.16
			112	0.49	936	90	268	223	1 157	22.8	21.8	5.61	0.62	0.14	0.16
			114	0.53	733	105	326	467	1 603	22.8	21.9	4.44	0.45	0.13	0.17
			137	0.46	848	73	165	341	1 208	21.1	20.7	5.33	0.59	0.16	0.16
			139	0.47	887	88	192	284	1 148	21.9	20.7	5.25	0.61	0.13	0.16
			141	0.48	726	67	167	241	878	21.5	21.5	4.86	0.60	0.16	0.16
			170	0.50	809	87	263	241	1 445	22.6	22.0	5.29	0.58	0.13	0.18
			172	0.53	883	79	644	n.d.	17 595	n.d.	17.8	5.37	0.55	0.14	0.94
			174	0.51	858	100	279	253	1 752	22.0	21.5	5.26	0.58	0.11	0.21
			197	0.50	926	119	320	252	1 963	23.7	22.5	5.66	0.57	0.10	0.19
			199	0.46	883	112	360	340	1 975	22.7	13.0	5.34	0.52	0.13	0.32
			201	0.47	728	111	321	374	1 663	22.8	10.0	4.74	0.47	0.12	0.25
			230	0.45	768	113	279	371	1 336	22.8	22.3	4.61	0.50	0.12	0.18
			232	0.47	680	121	388	399	1 594	23.2	22.6	4.73	0.43	0.11	0.17
			234	0.50	806	120	369	327	1 631	22.5	22.0	5.03	0.50	0.11	0.20

Note: n.d. represents not determined.

Table A2. Variation ranges and the average values of TOC normalized contents of odd *n*-alkanes (C_{27}+C_{29}+C_{31} *n*-alkanes) (ng/g TOC), total marine phytoplankton biomarkers (brassicasterol+dinosterol+C_{37} alkenones) (ng/g TOC), total *iso*-GDGTs (GDGT-0 to -3, Crenarcheol and Cre-isomer) (ng/g TOC) and $U^{K'}_{37}$-SST (°C), TEX_{86}-SST (°C), $1/P_{mar\text{-}aq}$, TMBR, BIT, MI indexes

Core		Odd *n*-alkanes (C_{27}+C_{29}+C_{31} *n*-alkanes)/ng·g^{-1} TOC	Brassicasterol+ Dinosterol+Alkenones/ng·g^{-1} TOC	$1/P_{mar\text{-}aq}$	TMBR	BIT	*iso*-GDGTs/ng·g^{-1} TOC*	MI*	$U^{K'}_{37}$-SST/°C	TEX_{86}-SST/°C*
MD052911	minimum	688	844	2.19	0.28	0.03	1 296	0.19	20.5	19.7
	maximum	1 215	2 123	3.06	0.52	0.06	5 463	0.38	25	29.3
	average	971	1 598	2.6	0.38	0.04	3 527	0.25	23.8	23.4
ORI-860-22	minimum	1 387	988	4.44	0.43	0.1	1 843	0.16	20.8	10
	maximum	2 126	1 987	5.76	0.65	0.18	4 254	0.32	23.7	22.6
	average	1 674	1 343	5.05	0.56	0.14	2 881	0.19	22.8	20.4

Note: * The abnormal values of *iso*-GDGTs, MI and TEX_{86}-SST at 172 cm depth in Core ORI-860-22 were ignored.